perfusion in a subset of patients conforms to this hypothesis. Because the use of HMPAO precludes the determination of absolute perfusion, the distinct possibility remains that a global CBF deficit, including the cerebellum, can occur during TGA. Further imaging studies, specifically with PET, are needed to elucidate the chain of events that elicit TGA.

ACKNOWLEDGEMENTS

We thank Amersham Buchler Healthcare, Braünschweig, Germany, whose financial support enabled the color reproduction of the SPECT images included in this article.

REFERENCES

1. Hodges JR. *Transient amnesia. Clinical and neuropsychological aspects.* London: W. B. Saunders; 1991:34.
2. Goldenberg G. Transient global amnesia. In: Baddeley AD, Wilson BA, Watts FN, eds. *Handbook of memory disorders.* Chichester, United Kingdom: John Wiley & Sons Ltd.; 1995:109–133.
3. Caplan LR. Transient global amnesia. In: Vinken PJ, Bruyn GW, Klawans HL, eds. *Handbook of clinical neurology,* Vol. 1. Amsterdam: Elsevier Scientific Publishers; 1985:205–218.
4. Hodges JR, Warlow CP. Syndromes of transient amnesia: towards a classification. A study of 153 cases. *J Neurol Neurosurg Psychiatry* 1990;53:834–843.
5. Bartenstein P, Ludolph A, Schober O, et al. Benzodiazepine receptors and cerebral blood flow in partial epilepsy. *Eur J Nucl Med* 1991;18:111–118.
6. Schubinger PA, Hasler PH, Beer-Wohlfarth H, et al. Evaluation of a multi-center study with iomacenil, a benzodiazepine receptor ligand. *Nucl Med Commun* 1991;12:569–582.
7. Lassen NA, Andersen AR, Neirinckx RD, Ell PJ, Costa DC. Validation of Ceretec. In: Ell PJ, Costa DC, Cullum ID, Jarritt PH, Lui D, eds. *rCBF atlas: the clinical application of rCBF imaging by SPECT.* High Wycombe, United Kingdom: Brier Press; 1987;14–18.
8. Inugami A, Kanno I, Uemura K, et al. Linearization correction of ^{99m}Tc-labeled hexamethyl-propylene amine oxime (HM-PAO) image in terms of regional CBF distribution: comparison to $C^{15}O_2$ inhalation steady-state method measured by positron emission tomography. *J Cereb Blood Flow Metab* 1988;8(suppl):S52–S60.
9. Yonekura Y, Nishiwaka S, Mukai T, et al. SPECT with [^{99m}Tc]-d,l-hexamethyl-propylene amine oxime (HM-PAO) compared with regional cerebral blood flow measured by PET: effects of linearization. *J Cereb Blood Flow Metab* 1988;8(suppl): S82–S89.
10. Martinot J, Hardy P, Feline A, et al. Left prefrontal glucose hypometabolism in the depressed state: a confirmation. *Am J Psychiatry* 1990;147:1313–1317.
11. Sackheim HA, Prohovnik I, Mueller JR, Mayeux R, Stern Y, Devanaud DP. Regional cerebral blood flow in mood disorders. II. Comparison of major depression and Alzheimer's disease. *J Nucl Med* 1993;34:1090–1101.
12. Schlegel S, Aldenhoff JB, Eischer D, Lindner P, Nickel O. Regional cerebral blood flow in depression: associations with pathophysiology. *J Affective Dis* 1989;17:211–218.
13. Stillhard G, Landis T, Schiess R, Regard M, Sialer G. Bitemporal hypoperfusion in transient global amnesia: 99-m-Tc-HM-PAO SPECT and neuropsychological findings during and after an attack. *J Neurol Neurosurg Psychiatry* 1990;53:339–342.
14. Evans J, Wilson B, Wraight EP, Hodges JR. Neuropsychological and SPECT scan findings during and after transient global amnesia: evidence for the differential impairment of remote episodic memory. *J Neurol Neurosurg Psychiatry* 1993;56: 1227–1230.
15. Tanabe H, Hashikawa K, Nakagawa Y, et al. Memory loss due to transient hypoperfusion in the medial temporal lobes including hippocampus. *Acta Neurol Scand* 1991;84:22–27.
16. Lin KN, Liu RS, Yeh TP, Wang SJ, Liu HC. Posterior ischemia during an attack of transient global amnesia. *Stroke* 1993;24:1093–1095.
17. Goldenberg G, Podreka I, Pfaffelmeyer N, Wessely P, Deecke L. Thalamic ischemia in transient global amnesia: a SPECT study. *Neurology* 1991;41:1748–1752.
18. Ohnishi T, Hoshi H, Nagamachi S, et al. High-resolution SPECT to assess hippocampal perfusion in neuropsychiatric disease. *J Nucl Med* 1995;36:1163–1169.
19. Sakashita Y, Sugimoto T, Taki S, Matsuda H. Abnormal cerebral blood flow following transient global amnesia (letter). *J Neurol Neurosurg Psychiatry* 1993;56:1327.
20. Hodges JR. Semantic memory and frontal executive function during transient global amnesia. *J Neurol Neurosurg Psychiatry* 1994;57:605–608.
21. Matsuda H, Higashi S, Tsuji S, et al. High resolution Tc-99m HMPAO SPECT in a patient with transient global amnesia. *Clin Nucl Med* 1993;18:46–49.
22. Trillet M, Croisile B, Philippon B, Vial C, Laurent B, Guillot M. Ictus amnésique et débits sanguins cérébraux. *Rev Neurol* 1987;143:536–539.
23. Crowell GF, Stump DA, Biller J, McHenry LC, Toole JF. The transient global amnesia–migraine connection. *Arch Neurol* 1984;41:75–79.
24. Baron JC, Petit-Taboué MC, Le Doze F, Desgranges B, Ravenel N, Marchal G. Right frontal cortex hypometabolism in transient global amnesia. A PET study. *Brain* 1994;117:545–552.
25. Laloux P, Brichant C, Cauwe F, Decoster P. Technetium-99m HM-PAO single photon emission computed tomography imaging in transient global amnesia. *Arch Neurol* 1992;49:543–546.
26. Volpe BT, Herscovitch P, Raichle ME, Hirst W, Gazzaniga MS. Cerebral blood flow and metabolism in human amnesia. *J Cereb Blood Flow Metab* 1983;3(suppl 1):S5–S6.
27. Olesen J, Balslev Jorgensen M. Leao's spreading depression in the hippocampus explains transient global amnesia. *Acta Neurol Scand* 1986;73:219–220.

Correlations Between Uptake of Technetium-99m Q12 and Thallium-201: Myocardial Perfusion and Viability in a Model of Acute Coronary Reperfusion

Norio Takahashi, Christopher P. Reinhardt, Robin Marcel and Jeffrey A. Leppo

Myocardial Isotope Research Laboratory and Departments of Medicine and Nuclear Medicine, University of Massachusetts Medical Center, Worcester, Massachusetts

To investigate whether Q12 uptake is affected by myocardial viability, as has been noted for ^{201}Tl and sestamibi, we analyzed the initial and delayed distribution patterns of Q12 in a rat coronary artery occlusion–reperfusion model. **Methods:** Animals were intubated and ventilated, and their arterial pressures were monitored. A left thoracotomy was performed. After a 1-hr occlusion and a 1-hr reperfusion of a major branch of the circumflex artery, ^{201}Tl and Q12 were injected intravenously. Radiolabeled microspheres were used to document the areas of risk and reperfusion. The animals were killed at 5 min or 1 hr after administration of the diffusible tracers. Tracer distribution was determined by segmental tissue analysis, and tissue viability was determined by histochemical staining. **Results:** Both the initial uptake and delayed retention of Q12 are sensitive to myocardial viability as shown by significantly lower uptake (28% ± 8%) and retention (41% ± 13%) of Q12 in the nonviable as compared to the viable segments ($p < 0.001$). In addition, the myocardial retention of Q12 was significantly less in the nonviable tissue when compared to the initial uptake ($p < 0.01$). **Conclusion:** The clinical implication of these observations suggests that initial and delayed imaging after Q12 administration would reflect both the initial regional blood flow pattern and myocardial viability. Also, delayed imaging of Q12 may reflect viability better than the initial imaging.

Key Words: technetium-99m Q12; myocardial viability; ischemia; coronary artery disease; thallium-201

J Nucl Med 1998; 39:159–165

Received Oct. 18, 1996; accepted Mar. 14, 1997.

For correspondence or reprints contact: Jeffrey A. Leppo, MD, Department of Nuclear Medicine, University of Massachusetts Medical Center, 55 Lake Avenue North, Worcester, MA 01655-0243.

Stress ^{201}Tl myocardial perfusion imaging is widely used for the scintigraphic evaluation of coronary artery disease (*1–3*). However, ^{99m}Tc-labeled sestamibi has shown a diagnostic ability that is similar to that of ^{201}Tl (*4*). As a result, sestamibi is now commonly used to evaluate coronary artery disease. Given the improved imaging characteristics afforded by the ^{99m}Tc label and the early experimental and clinical success of sestamibi, research into the development of additional ^{99m}Tc-labeled myocardial imaging agents continues.

Trans-(1,2-bis(dihydro-2,2,5,5-tetramethyl-3(2H)furanonate-4-methyleneimino)ethane)bis(tris(3-methoxy-1-propyl)phosphine) ^{99m}Tc(III) (known as Q12) is a recently developed myocardial perfusion agent (*5*). Using a canine model, Gerson et al. (*6*) demonstrated that the clearance rates of Q12 are the same from normal and ischemic myocardium. In addition, a human volunteer study has shown minimal 5-hr clearance (*5*), thereby potentially allowing for clinical imaging several hours after administration.

Previous studies have demonstrated that the myocardial distributions of sestamibi and ^{201}Tl are affected by myocardial viability (*7–9*), and this property may be important in the early detection of myocardial infarction. Like sestamibi, Q12 is a lipophilic cation (*5*), and it is possible that they both share similar cardiac transport properties. Therefore, we hypothesized that the cardiac transport of Q12 would also be affected by tissue viability and that initial Q12 myocardial uptake would be relatively stable over time.

To evaluate these hypotheses, we compared the initial and delayed distribution patterns of Q12 in a rat model that is designed to simulate the clinical problem of assessing flow and viability after successful thrombolysis or reperfusion in an evolving myocardial infarct or acute ischemic event. The distribution pattern of Q12 was then compared with that of simultaneously injected ^{201}Tl. A previous study (*9*) used ^{99m}Tc-sestamibi and tetrofosmin in a similar model and would serve as a useful comparison with the ^{99m}Tc/Q12 results described here.

MATERIALS AND METHODS

Radiopharmaceutical Preparation

Mallinckrodt, Inc. (St. Louis, MO) supplied Q12 as an "instant kit." Each vial was reconstituted with 2–3 ml of ^{99m}Tc as sodium pertechnetate containing no more than 100 mCi of ^{99m}Tc. The vial was placed in a boiling water bath for 15 min and then cooled to room temperature. Radiochemical purity was tested using Sep-Pak Alumina cartridges (Millipore Corp., Milford, MA), as described previously (*10*). Radiochemical purity values ranged from 95% to 97%. Within 1 hr after chemical preparation, Q12 was injected in the animals. It has been reported that radiochemical purity remains unchanged for at least 8 hr (*5*). In addition, we repeated this quality control measurement at the conclusion of each experiment and noted no significant change in Q12 purity.

Surgical Preparation

Sprague-Dawley male rats (n = 14, 300–600 g; Taconic Farms, Germantown, NY) were sedated with intramuscular ketamine (0.14 mg/g) and xylazine (0.035 mg/g) and then anesthetized with 0.5%–2.0% isoflurane administered through an anesthesia apparatus (Ohio model 7000; Ohio Medical, Cleveland, OH). Ventilatory parameters and supplemental oxygen were adjusted to maintain physiological arterial blood gases. The carotid artery was catheterized, and arterial pressure was recorded continuously (Linearcorder WR3101; Graphtec Corp., Irvine, CA). A femoral artery and vein were isolated and cannulated for withdrawal of arterial blood samples (microsphere references and blood gases) and for administration of Q12 and ^{201}Tl, respectively. The heart was exposed in a pericardial cradle through a left thoracotomy, and a catheter was placed in the left atrium for the injection of radiolabeled microspheres.

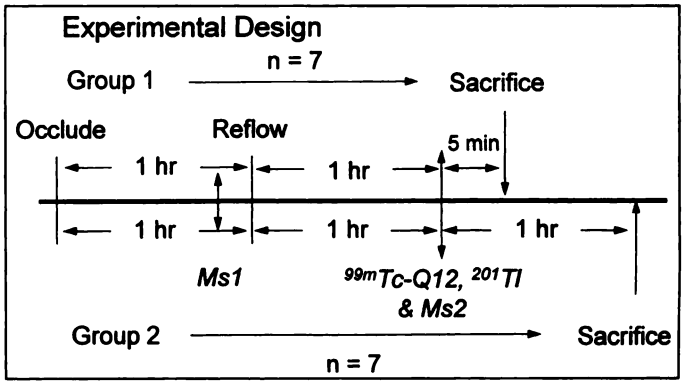

FIGURE 1. Schematic representation of the experimental design. Ms1, first set of microspheres; Ms2, second set of microspheres. Group 1 represents the initial tracer distribution pattern, whereas Group 2 represents the delayed distribution pattern.

Experimental Protocol

The experimental design is shown schematically in Figure 1. Severe regional hypoperfusion was induced by occlusion of a major branch of the left circumflex artery for 1 hr. After 55 min of occlusion, the first set of microspheres (^{95}Nb, 5×10^5, 12–15 mm) was injected through a left atrial catheter (*11*). Simultaneously, a 2-min reference blood sample was drawn at a rate of 0.97 ml/min from a femoral arterial catheter using an infusion pump (Harvard Apparatus, Millis, MA). After 1 hr of reperfusion, ^{99m}Tc-labeled Q12 (5 mCi) and ^{201}Tl (250 mCi) were administered (*11,12*). Immediately after administration of the tracers, a second set of microspheres (^{103}Ru, 5×10^5, 12–15 mm) was injected, and the reference blood sample was withdrawn for 2 min to document the extent of reperfusion flow. The tracers were allowed to circulate for 5 min (Group 1, n = 7) to evaluate initial distribution or 1 hr (Group 2, n = 7) to assess delayed distribution after which the rats were killed.

Postmortem Analysis

The hearts were excised and then frozen to allow for uniform sectioning. Transmural left ventricular segments were collected and weighed (32–40 segments per heart). The average left ventricle and sample weights were 1.09 ± 0.11 g and 0.03 ± 0.01 g, respectively. Because histochemical stains have been shown to affect the postmortem distribution of ^{201}Tl (*9,13*), each thawed segment was incubated separately in a bath of nitroblue tetrazolium (NBT) (1 ml in 0.05% phosphate-buffered solution; pH 8.0) at 37°C. On the basis of histochemical results, segments were classified as viable (100% blue stain) or nonviable [mosaic (mix of pale and blue stain) or infarct (100% pale)].

The tissue segments were then removed from the histochemical buffer and placed in separately labeled test tubes. The tissue samples, along with the NBT solution and arterial blood samples, were then counted in a NaI (Tl) gamma well scintillation counter (Auto-Gamma 5530; Packard Instrument Company, Downers Grove, IL). Any postmortem tracer activity loss associated with the NBT incubation was accounted for by a separate activity measurement of the tissue and NBT bath. All samples were corrected for interradionuclide cross-over and tracer decay during the counting period. Tracer activity concentration was expressed as dpm/g.

Absolute Myocardial Blood Flow

Absolute myocardial blood flow (ml/min/g) was determined, as described previously (*14*). Briefly, the myocardial microsphere density in each segment (dpm/g) was determined, and the microsphere content in the 2-min reference blood collection (dpm/ml/min) was then used to calculate absolute flow (dpm/g ÷ dpm/ml/min).

TABLE 1
Hemodynamic Measurement

Group	Heart rate (beats/min)			Peak systolic pressure (mmHg)		
	Baseline	Occlusion	Reflow	Baseline	Occlusion	Reflow
1	203 ± 17	207 ± 16	211 ± 16	84 ± 6	74 ± 5*	73 ± 10*
2	204 ± 12	207 ± 28	215 ± 38	87 ± 10	73 ± 9*	76 ± 11*

*$p < 0.05$ compared to baseline

Tracer Activity Concentration (Relative Concentration)

The relative blood flow in each segment (dpm/g) was also normalized to the average left ventricular activity concentration (dpm/g), as defined by the following equation:

$$\Sigma_{LV}A/\Sigma_{LV}m,$$

where $\Sigma_{LV}A$ and $\Sigma_{LV}m$ represent the total tracer activity and total mass of the left ventricle, respectively. Then the microsphere content for each segmental tissue sample could be expressed as a relative concentration (RC) (*15,16*) as compared to the average left ventricular activity concentration. We also used a similar normalization procedure for ^{201}Tl and Q12 so that the RC values for each tracer could be compared over a similar range. In these analyses, a value of 1.0 represents unity and is the average activity concentration of any specific isotope in the myocardium. Therefore, RC values above 1.0 define higher flow or diffusible tracer content, whereas values below 1.0 have low flow or tracer content as compared to the average left ventricular concentration.

Tissue Retention After Histochemical Staining

To evaluate the effect of NBT staining on the distribution of each diffusible tracer, we measured the tissue retention (TR) in the viable and nonviable region:

TR = Tissue activity/(tissue activity
+ corresponding NBT buffer solution activity) × 100%.

Statistical Analysis

All data are presented as mean ± s.d. Univariate analysis of groups was performed by a paired Student's t-test, unpaired two-sample Student's t-test, Wilcoxon signed rank test or Wilcoxon rank-signed test. An analysis of variance and Bonferroni Student's t-test were used when multiple comparisons were made as a function of time. Analysis of variance was also performed in comparison of regression lines. All of these statistical calculations were performed using a commercially available computer program (Sigma Stat, Jandel Corporation; or Stata, Stata Corporation).

RESULTS

Hemodynamics

Hemodynamic variability in heart rate and peak systolic pressure during baseline, occlusion and reperfusion periods are shown in Table 1. All groups showed stability in heart rate during the experimental protocol. Peak systolic pressure fell slightly as compared to baseline during occlusion and reperfusion in both groups. There were no significant differences in heart rate and blood pressure between groups.

Measurement of Myocardial Blood Flow

To simplify the comparison of the tracer uptake in the viable and nonviable myocardium, all individual segments were placed into one of four categories based on normalized reperfusion measurements as shown in Table 2. We used a lowest flow region, represented by <0.75 of average left ventricular reperfusion flow; a lower flow reduction, defined by a flow level of 0.75–0.99; a higher flow, classified by a normalized level of 1–1.25; and a highest flow level, defined by >25% of average flow. This division into four sequential subgroups of lowest to highest reperfusion flow permitted us to evaluate the effect of viability on tracer content independently of variations in regional blood flow. Given the small number of mosaic segments, mosaic and infarct segments were combined into one nonviable category.

TABLE 2
Comparison of Blood Flow, Thallium-201 and Q12 Distribution Based on Four Levels of Normalized Reperfusion Flow

	Normalized reflow (relative concentration)							
	<0.75 (lowest)		0.75–0.99 (lower)		1.0–1.25 (higher)		>1.25 (highest)	
	Viable	Nonviable	Viable	Nonviable	Viable	Nonviable	Viable	Nonviable
Group 1								
No. of segments	3	21	65	25	71	33	9	12
Occ (ml/min/g)	1.65 ± 0.65	0.24 ± 0.35*	2.38 ± 0.41	0.64 ± 0.61*	2.71 ± 0.42	0.98 ± 0.72*	2.92 ± 0.45	1.00 ± 0.57*
Occ (RC)	0.80 ± 0.23	0.13 ± 0.19*	1.28 ± 0.22	0.36 ± 0.34*	1.47 ± 0.21	0.51 ± 0.36*	1.67 ± 0.31	0.56 ± 0.32*
Rep (ml/min/g)	2.17 ± 0.41	1.39 ± 0.38†	2.34 ± 0.57	1.97 ± 0.40†	2.70 ± 0.65	2.88 ± 0.71	2.75 ± 0.61	3.12 ± 0.68
Rep (RC)	0.73 ± 0.01	0.63 ± 0.08‡	0.92 ± 0.06	0.88 ± 0.07§	1.10 ± 0.07	1.12 ± 0.07	1.35 ± 0.07	1.33 ± 0.06
^{201}Tl (RC)	0.94 ± 0.03	0.53 ± 0.11*	1.10 ± 0.10	0.69 ± 0.16*	1.18 ± 0.11	0.92 ± 0.14*	1.27 ± 0.19	0.95 ± 0.08*
Q12 (RC)	0.96 ± 0.04	0.60 ± 0.12*	1.08 ± 0.09	0.76 ± 0.15*	1.16 ± 0.10	0.92 ± 0.11*	1.22 ± 0.17	0.95 ± 0.08*
Group 2								
No. of segments	6	15	65	21	81	37	7	12
Occ (ml/min/g)	1.67 ± 0.22	0.18 ± 0.34*	2.10 ± 0.48	0.37 ± 0.45*	2.38 ± 0.50	0.71 ± 0.60*	2.49 ± 0.69	0.98 ± 0.71*
Occ (RC)	1.07 ± 0.11	0.10 ± 0.16*	1.24 ± 0.23	0.25 ± 0.30*	1.38 ± 0.21	0.43 ± 0.34*	1.59 ± 0.41	0.56 ± 0.39*
Rep (ml/min/g)	1.78 ± 0.75	1.16 ± 0.28§	2.55 ± 0.89	1.89 ± 0.25*	2.70 ± 0.94	2.92 ± 0.99	3.34 ± 1.06	3.88 ± 1.28
Rep (RC)	0.66 ± 0.07	0.55 ± 0.13	0.91 ± 0.07	0.85 ± 0.07†	1.10 ± 0.06	1.11 ± 0.08	1.37 ± 0.12	1.38 ± 0.15
^{201}Tl (RC)	1.10 ± 0.10	0.52 ± 0.15*	1.08 ± 0.11	0.64 ± 0.15*	1.17 ± 0.10	0.81 ± 0.14*	1.24 ± 0.18	0.93 ± 0.15*
Q12 (RC)	1.11 ± 0.08	0.48 ± 0.13*	1.09 ± 0.14	0.60 ± 0.16*	1.19 ± 0.12	0.78 ± 0.15*	1.23 ± 0.24	0.90 ± 0.13†

*$p < 0.001$ compared to viable.
†$p < 0.01$ compared to viable.
‡$p < 0.05$ compared to viable.
§$p < 0.02$ compared to viable.
Rep = reperfusion blood flow; Occ = occlusion blood flow; RC = relative concentration (activity of segment/weight of segment)/(activity of whole ventricle/weight of whole ventricle).

In each of the four subgroups, RC values are displayed for viable and nonviable segments, as well as for occlusion and reperfusion flow. As expected, both the absolute (ml/min/g) and normalized occlusion blood flow in the nonviable segments were significantly lower than those noted for the viable segments at all flow levels of both groups. In addition, we documented successful reperfusion because the absolute blood flow during reperfusion increased significantly, as compared to the flow during occlusion in the nonviable segments in all four subgroups ($p < 0.001$). In the viable segments, the absolute blood flow during reperfusion significantly increased ($p < 0.01$) or was stable, as compared to that during occlusion. The absolute reperfusion blood flow was not statistically different between Groups 1 and 2 at all flow levels.

Myocardial Distribution of Thallium-201, Q12 and Reperfusion Blood Flow Between Viable and Nonviable Segments

As displayed in Table 2, the reperfusion blood flow in most subgroups at the time of diffusible tracer administration was similar between the viable and nonviable segments. In contrast, the mean activity concentration of diffusible tracers was significantly lower in all the nonviable segments, as compared to the viable segments. Therefore, as shown in Figure 2, this decrease in tracer uptake and retention in both groups cannot be explained by regional flow differences. Specifically, in Group 1, the activity concentration of Q12 in the nonviable segments was 38% lower in the lowest flow group and 30% less in the lower flow segments as compared to Q12 activity in the viable segments. At the higher and highest flow levels, there was a mean Q12 reduction of 21% in the nonviable higher flow segments and a 22% reduction in the highest flow segments.

Similar findings were observed in Group 2. Q12 activity concentration in the nonviable segments was reduced by 57% in the lowest flow group and by 45% in the lower flow group. In addition, Q12 activity concentration in the nonviable segments was 34% less in the higher and 27% less in the highest flow segments as compared to viable segments.

In an analogous fashion, ^{201}Tl activity concentration in the nonviable segments was significantly lower than that noted for the viable segments in both groups at all flow levels. This observation demonstrates that both the initial and delayed distribution of Q12 and ^{201}Tl are affected by myocardial viability.

Myocardial Distribution of Thallium-201 and Q12 Between Groups 1 and 2

The normalized reperfusion blood flow was not statistically different between Groups 1 and 2, except in the nonviable segments at lowest flow level ($p < 0.05$). Overall, there was only a 4% difference in viable and nonviable normalized reperfusion flow. In contrast, the average differences in Q12 content between the viable and nonviable segments were 28% in Group 1 and 41% in Group 2. These findings suggest that there was preferential loss of myocardial Q12 activity in the nonviable myocardium 1 hr after administration.

Similarly, the net retention of ^{201}Tl (Group 2) was lower than the initial uptake (Group 1) in the nonviable segments, but the difference only reached statistical significance at the higher flow level ($p < 0.01$). The average differences in ^{201}Tl activity concentration between the viable and nonviable segments were 32% in Group 1 and 37% in Group 2. These findings also suggest that there is preferential loss of ^{201}Tl in nonviable myocardium, but it appears that the loss of Q12 from nonviable myocardium is more prominent.

Figure 3A shows the correlation of Q12 as a function of reperfusion blood flow for Groups 1 and 2. The slope and intercept for the Group 1 and 2 hearts show essentially no change. This suggests that Q12 does not undergo tracer redistribution during the time course of this protocol.

In contrast to Q12, the slope for the regression lines of ^{201}Tl from Group 2 was lower (and intercept was higher) than that of Group 1, as displayed in Figure 3B. This significant ($p < 0.02$) difference in the slope of the nonviable segments suggests that there is ^{201}Tl redistribution during 1 hr of tracer recirculation. In addition, this loss of tracer from the nonviable segments may be reduced at the lower and lowest flow levels.

Effect of Nitroblue Tetrazolium Staining on the Distributions of Thallium-201 and Q12

Table 3 shows the TR rate for ^{201}Tl and Q12 in the viable, mosaic and infarct regions. In both Group 1 and 2 hearts, the TR of ^{201}Tl in the nonviable region (mosaic and infarct) was significantly higher than that noted for the viable region. In contrast, the TR of Q12 in the nonviable region was significantly lower than that noted for the viable region. In addition, we noticed that the TR of ^{201}Tl was approximately 50% of the value of Q12.

DISCUSSION

This study shows that both the initial (5-min) uptake and delayed retention of Q12 and ^{201}Tl are affected by the status of myocardial viability. This was demonstrated by significantly lower uptake and retention values for ^{201}Tl and Q12 when the nonviable segments were compared with the viable segments at all flow levels. In addition, this study suggests that the Q12 has a more stable myocardial distribution pattern over time than does ^{201}Tl and does not display appreciable tracer redistribution.

Interaction of Viability and Tracer Uptake

The finding that Q12 uptake is affected by myocardial viability is consistent with observations in an isolated rat heart study (*10*). Although the myocellular mechanism(s) associated with the uptake and retention of Q12 are as yet unknown, several prior investigations into the cellular mechanisms governing the retention of sestamibi and ^{201}Tl have been reported. Specifically, Piwnica-Worms et al. (*17*) showed that sestamibi transport involves passive diffusion across the plasma and mitochondrial membranes, and it is sequestered largely within mitochondria by the large negative transmembrane potentials. When plasma or mitochondrial membrane potentials are depolarized secondary to irreversible myocardial injury, there is an inhibition in net uptake of sestamibi and, thereby, a reduction in myocyte retention. Given the similar lipophilic cation nature and composition of Q12 (*5*), it may also be inhibited by similar mechanisms that have been noted for sestamibi. We previously reported that sestamibi uptake was lower in the nonviable as compared to the viable segments in a similar model to that presented here (*9*). We also noted that both sestamibi (*9*) and Q12 show higher tracer retention in nonviable tissue after histochemical staining techniques. Overall, these observations in our prior (*9*) and current experiments support a common transport mechanism for these two ^{99m}Tc perfusion tracers.

Although both uptake and retention of Q12 and ^{201}Tl were depressed in the nonviable segments compared to the viable segments, the activity concentration of both tracers displays linear uptake as flow increases, which is independent of viability. This same trend was observed in the other cationic perfusion tracers, ^{99m}Tc-tetrofosmin (tetrofosmin) and sesta-

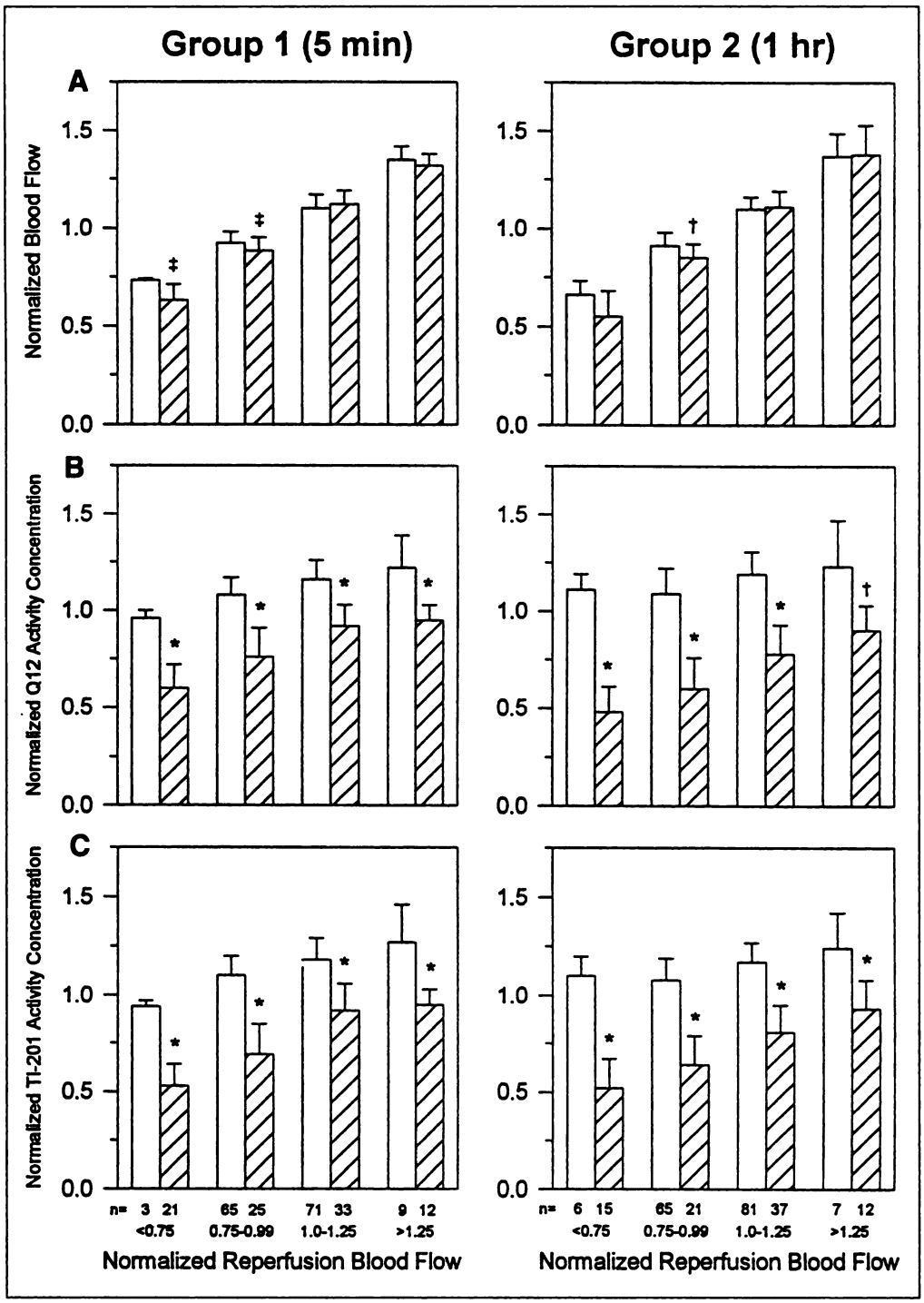

FIGURE 2. Bar graphs display normalized reperfusion blood flow (A), Q12 (B) and ^{201}Tl (C) activity concentration, which compare the viable (□) and nonviable (▨) segments in relation to the four levels of normalized reperfusion blood flow, from the lowest (RC < 0.75) to the highest (RC > 1.25) subgroup. The number (n) of individual segments in each subgroup is shown just below each bar in the graph. *$p < 0.001$; †$p < 0.01$; ‡$p < 0.05$ compared to viable.

mibi (*9*). Because these tracers are affected by both flow and myocardial viability, perfusion defects could result from either viable areas that are hypoperfused or nonviable tissue that are receiving normal basal flow. Therefore, in clinical situations that involve imaging during coronary occlusion and reperfusion, these tracers should be used after reactive hyperemia has abated to help evaluate the relationship between myocardial viability and regional blood flow.

Myocardial Tracer Stability

In Group 2 hearts, which experience 1 hr of tracer recirculation, Q12 activity is preferentially lost from the nonviable myocardium at all flow levels. This result is consistent with isolated heart experiments that demonstrated biphasic myocardial clearance of Q12 with a fast early and slow late phase (*10,18*). An accelerated early rapid clearance phase in nonviable myocardium was also noted (*10*). The observation that Q12 does not show myocardial redistribution is also consistent with a recent canine study (*6*).

Effect of Nitroblue Tetrazolium Staining on Q12 and Thallium-201 Distribution

The postmortem incubation of myocardium with NBT was associated with tracer washout for both Q12 and ^{201}Tl. Our group previously reported that the postmortem distribution of ^{201}Tl and sestamibi are affected by triphenyl tetrazolium chlo-

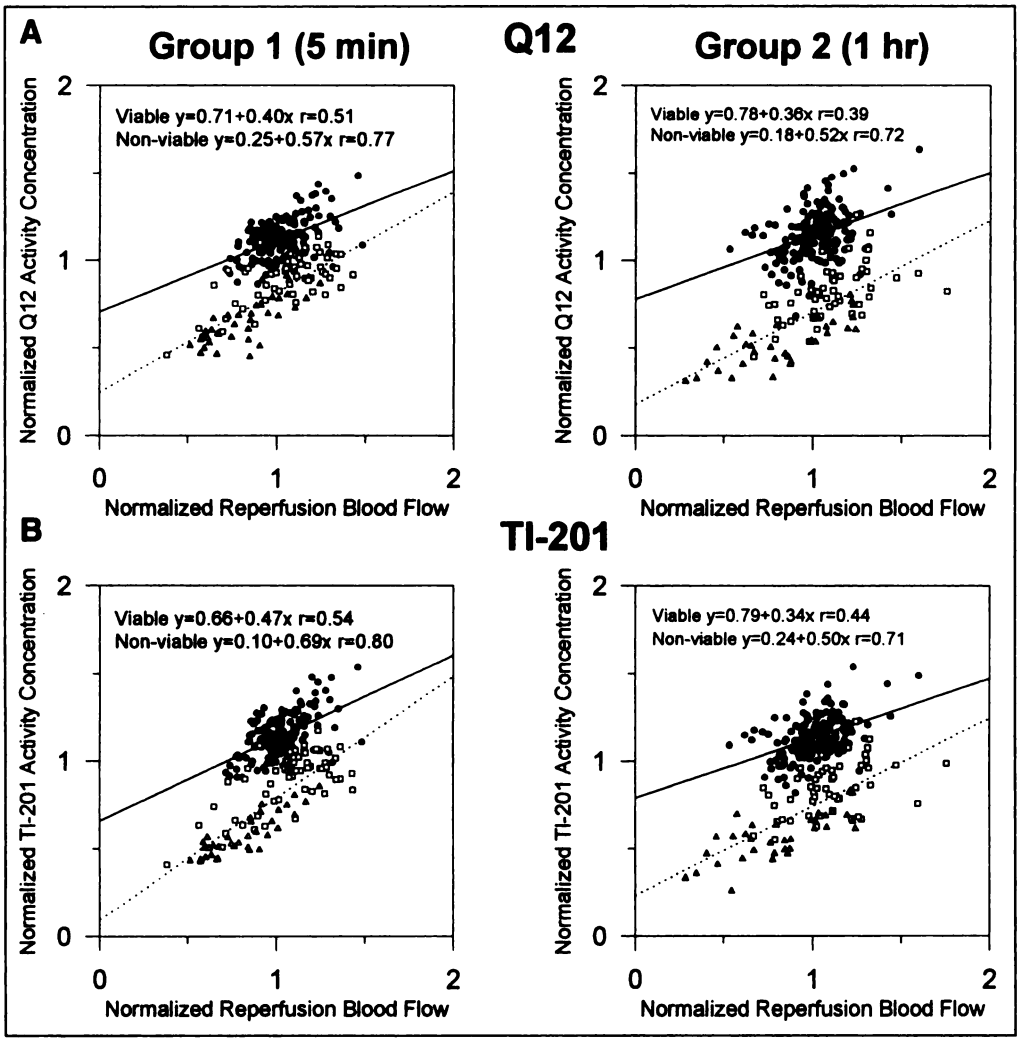

FIGURE 3. Individual segments from all Group 1 and 2 hearts are shown. The normalized reperfusion blood flow was plotted against its normalized (RC) Q12 (A) and ^{201}Tl (B) activity concentration for both the viable (●) and nonviable (□, mosaic; △, infarct) myocardial segments. The least square linear regression lines (solid line represents the viable segments, whereas dotted line represents the nonviable segments) and equations are also shown.

ride (*13*). In addition, we have reported that NBT staining can affect the postmortem myocardial distribution of ^{201}Tl, sestamibi and tetrofosmin. The current observation with Q12 is consistent with previous reports concerning sestamibi and tetrofosmin (*9,19*). If we had not accounted for the possible effect of postmortem tracer washout, we might have overestimated the effect of viability on myocardial Q12 uptake. In contrast, NBT exposure results in an increased loss of ^{201}Tl from viable cells that, if uncorrected, could have caused an underestimation of the effect of viability on ^{201}Tl kinetics.

Overall, our observations that histochemical staining has an effect on tracer retention in postmortem tissue suggest that there are differences in the intracellular binding properties of ^{201}Tl and Q12. This could involve a possible NBT effect on the ^{99m}Tc label stability as well as potential differences in the subcellular localization in parenchymal cell binding sites. Clearly, further specific investigations in this area are warranted.

Limitations

There are several important limitations to note:

1. This study did not assess serial tracer changes over time in the same group of rats. However, both the absolute and normalized reperfusion blood flow rates in Groups 1 and 2 were statistically similar at all but one flow level (nonviable segments, lowest flow level). The design limitation also precluded paired Student's t-test comparisons, but we were still able to show consistent and significant differences in tracer uptake and retention among the viable and nonviable segments.

TABLE 3
Comparison of Tissue Retention of Thallium-201 and Q12 after Nitroblue Tetrazolium Staining

	Group 1 (5 min)			Group 2 (1 hr)		
	Viable	Mosaic	Infarct	Viable	Mosaic	Infarct
^{201}Tl	35.2 ± 7.0	37.4 ± 7.2*	43.7 ± 8.3†‡	32.6 ± 2.7	37.6 ± 4.3†	48.2 ± 7.9‡§
Q12	74.2 ± 1.1	71.5 ± 0.6§	70.3 ± 2.4§	75.6 ± 1.6	72.9 ± 2.0§	70.1 ± 1.7‡§

*$p < 0.02$ compared to viable.
†$p < 0.01$ compared to viable.
‡$p < 0.01$ compared to mosaic.
§$p < 0.001$ compared to viable.

2. The 1-hr time course of delayed tracer distribution may appear relatively short. However, the normal heart rate in rats is about 3-fold higher than that in humans, and 1 hr is a sufficient time period to evaluate for redistribution.
3. Although we confirmed our hypothesis that the cardiac transport of Q12 would be affected by myocardial viability, we have not particularly addressed the mechanism of cellular uptake and retention. In addition, the accelerated Q12 washout from nonviable myocardium also needs further investigation, which was beyond the scope of this in vivo model.

CONCLUSION

We have observed that the myocardial uptake of Q12 is linearly related to regional blood flow and that the loss of tissue viability will accelerate tracer loss over time. Therefore, in clinical situations that involve coronary occlusion and reperfusion, such as acute myocardial infarctions and thrombolysis, the distribution of Q12 will be affected by myocardial viability. Specifically, delayed imaging after Q12 administration would probably reflect myocardial viability more clearly than do the initial images. Although we noted a depression of Q12 and ^{201}Tl uptake in the nonviable tissue, its impact on the highest flow regions is less than that noted in the very low flow regions. Further clinical trials including quantitative myocardial scan analysis will need to be performed to determine the impact of these basic observations on the evaluation of acute coronary ischemia and reperfusion.

ACKNOWLEDGMENTS

We are grateful to Mallinckrodt, Inc., for providing a research grant to partially support these experiments. We thank Harriet Kay for editorial assistance.

REFERENCES

1. Pohost GM, Zir LM, Moore RH, McKusick KA, Guiney TE, Beller GA. Differentiation of transiently ischemic from infarcted myocardium by serial imaging after a single dose of thallium-201. *Circulation* 1977;55:294–302.
2. Dilsizian V, Rocco TP, Freedman NMT, Leon MB, Bonow RO. Enhanced detection of ischemic but viable myocardium by the reinjection of thallium after stress-redistribution imaging. *N Engl J Med* 1990;323:141–146.
3. Gewirtz H, Beller GA, Strauss HW, et al. Transient defects of resting thallium scans in patients with coronary artery disease. *Circulation* 1979;59:707–713.
4. Wackers FJT, Berman DS, Maddahi J, et al. Technetium-99m hexakis 2-methoxy-isobutyl isonitrile: human biodistribution, dosimetry, safety and preliminary comparison to thallium-201 for myocardial perfusion imaging. *J Nucl Med* 1989;30:301–311.
5. Rossetti C, Vanoli G, Paganelli G, et al. Human biodistribution, dosimetry and clinical use of technetium(III)-99m-Q12. *J Nucl Med* 1994;35:1571–1580.
6. Gerson MC, Millard RW, Roszell NJ, et al. Kinetic properties of ^{99m}Tc-Q12 in canine myocardium. *Circulation* 1994;89:1291–1300.
7. Maddahi J, Ganz W, Hinomiya K, et al. Myocardial salvage by intracoronary thrombolysis in evolving acute myocardial infarction: evaluation using intracoronary injection of thallium-201. *Am Heart J* 1981;102:664–674.
8. Sinusas AJ, Trautman KA, Bergin JD, et al. Quantification of area at risk during coronary occlusion and degree of myocardial salvage after reperfusion with technetium-99m methoxyisobutyl nitrile. *Circulation* 1990;82:1424–1437.
9. Takahashi N, Reinhardt CP, Marcel R, Leppo J. Myocardial uptake of ^{99m}Tc-tetrofosmin, sestamibi and ^{201}Tl in a model of acute coronary reperfusion. *Circulation* 1996;94:2605–2613.
10. Okada RD, Nguyen KN, Lauinger M, et al. Effects of no flow and reperfusion on technetium-99m-Q12 kinetics. *J Nucl Med* 1995;36:2103–2109.
11. Reinhardt CP, Weinstein H, Leppo JA. Comparison of iodine-125-BMIPP and thallium-201 in myocardial hypoperfusion. *J Nucl Med* 1995;36:1645–1653.
12. Weinstein H, Reinhardt CP, Leppo JA. Teboroxime, sestamibi and thallium-201 as markers of myocardial hypoperfusion: comparison by quantitative dual isotope autoradiography in rabbits. *J Nucl Med* 1993;34:1510–1517.
13. Reinhardt CP, Weinstein H, Wironen J, Leppo JA. Effect of triphenyl tetrazolium chloride staining on the distribution of radiolabeled pharmaceuticals. *J Nucl Med* 1993;34:1722–1727.
14. Heyman MA, Payne BD, Hoffman JIE, Rudolph AM. Blood flow measurement with radionuclide-labeled particles. *Prog Cardiovasc Dis* 1977;20:55–79.
15. King RB, Bassingthwaighte JB, Hales JRS, Rowell LB. Stability of heterogeneity of myocardial blood flow in normal awake baboons. *Circ Res* 1985;57:285–295.
16. Yipintsoi T, Dobbs WA Jr, Scanlon PD, Knopp TJ, Bassingthwaighte JB. Regional distribution of diffusible tracers and carbonized microspheres in the left ventricle of isolated dog hearts. *Circ Res* 1973;33:573–587.
17. Piwnica-Worms D, Kronauge JF, Chiu ML. Uptake and retention of hexakis (2-methoxyisobutyl isonitrile) technetium(I) in cultured chick myocardial cells: mitochondrial and plasma membrane potential dependence. *Circulation* 1990;82:1826–1838.
18. McGoron AJ, Gerson MC, Biniakiewicz DS, Washburn LC, Millard RW. Effects of ouabain on technetium-99m-Q12 and thallium-201 extraction and retention by isolated rat heart. *J Nucl Med* 1996;37:752–756.
19. Villegas BJ, Reinhardt CP, Dahlberg ST, Marcel R, Heller LI, Leppo JA. Sestamibi distribution in viable and nonviable myocardium assessed independent of the effect of vital stains [Abstract]. *J Nucl Med* 1994;35:152.